J. Opt. B: Quantum Semiclass. Opt. **1** (1999) 357–363. Printed in the UK PII: S1464-4266(99)00651-5

A study of quantum decoherence via spontaneous emission in a system with Kolmogorov–Arnol'd–Moser tori

G H Ball, K M D Vant, H Ammann and N L Christensen

Department of Physics, University of Auckland, Auckland, New Zealand

Received 5 January 1999, in final form 11 February 1999

Abstract. We present an experimental and numerical study of the effects of decoherence on a quantum system whose classical analogue has Kolmogorov–Arnol'd–Moser (KAM) tori in its phase space. Atoms are prepared in a caesium magneto-optical trap at temperatures and densities which necessitate a quantum description. This real quantum system is coupled to the environment via spontaneous emission. The degree of coupling is varied and the effects of this coupling on the quantum coherence of the system are studied. When the classical diffusion through a partially broken torus is $\lesssim\hbar$, diffusion of quantum particles is inhibited. We find that increasing decoherence via spontaneous emission increases the transport of quantum particles through the boundary.

Keywords: Quantum chaos, decoherence, laser cooled atoms

1. Introduction

The study of decoherence in a quantum system has been a subject of much interest in recent years. Since the emergence of quantum mechanics some 70 years ago, a central problem in its interpretation has been the fact that the linearity of the Schrödinger equation allows macroscopic physical states to be derived from arbitrary superpositions of other states, a situation which is quite clearly in contradiction to our experience. This was originally illustrated in the familiar paradox of Schrödinger's cat. One simple explanation is to suppose that an initially classical state for a macroscopic system will always evolve into another classical state so that for a universe with a suitable initial condition, non-classical states occur only when carefully prepared by some experimentalist. In this interpretation, Schrödinger's cat presents no paradox but merely lies outside our normal realm of experience. This hypothesis can be rejected in the light of quantum analysis of real macroscopic, classically chaotic systems. Calculations (see, for example, Zurek's discussion in terms of celestial objects [1]) indicate that in these systems, quantum dynamics differ from classical after relatively short times, and lead to flagrantly non-classical states. Any successful theory must explain why these states are not found in practice.

A recent, successful explanation of the quantum–classical correspondence problem has been achieved through studies of the influence of decoherence [2, 3]. In this approach, any real, open quantum system leaks coherence to its surroundings via extraneous degrees of freedom which are coupled to the environment. The rate at which this decoupling proceeds depends on the particular state of the system, the dynamics of the system and the form of the interaction with the environment. In a measurement of a microscopic system by a macroscopic observer, the wavefunction collapse of traditional measurement theory is caused by decoherence of the meter entangled with the system. Bizarre macroscopic quantum states might in theory be prepared, but will survive only for a vanishingly short time, and the classical description of the world as we observe it will be regained. Quantum mechanics without fundamental modification retains its position as the true description of the universe, and the limited set of states which we observe around us is accounted for.

The study of the signatures of classical phase space structures in a quantum system is an important topic in quantum chaos. For a closed integrable system with two degrees of freedom, all solutions lie on tori embedded in four-dimensional phase space. Each solution or trajectory is indefinitely confined to its own torus. If the winding number for the torus is rational then the trajectories are periodic, whereas for an irrational winding number the motion in phase space is quasi-periodic. If the system Hamiltonian is perturbed such that it becomes non-integrable, nonlinear resonances appear in the phase space at the location of tori with rational winding numbers, altering the topology and destroying these tori. Trajectories which were confined on the vanished tori, now traverse the same general region of phase space. However the Kolmogorov–Arnol'd–Moser (KAM) theorem states that tori with irrational winding numbers (KAM tori) are not immediately destroyed by small amounts of non-integrability and continue to act as tori in the new phase space. For increasing perturbation, the nonlinear resonances grow and the KAM tori are eventually destroyed

by nearby resonances. Within a given region of phase space, those with the most irrational winding numbers are the last to break up [4]. When a KAM torus is destroyed, a *cantorus* is left in its place. The properties of a broken torus or cantorus in a quantum system have been the subject of considerable interest and several numerical studies [5–9].

In this paper, we study the effects of increasing the coupling of a quantum system to its environment. Our experimental system is a low density cloud of cold ($\sim$15 μK) caesium atoms prepared in the ultra-high vacuum glass cell of a magneto-optical trap (MOT). Because of the low densities achieved in a MOT, the interactions of the atoms are negligible and each atom can be modelled as a quantum particle in a periodic potential. With 10^5 atoms trapped per experimental run, we deal with statistically significant numbers of particles so the experimental distributions will closely approximate quantum probability distributions. We temporally modulate a standing wave optical potential which creates a classically chaotic system with KAM tori (impenetrable momentum barriers) in its phase space. For an increased Rabi frequency (i.e. increased perturbation), holes appear in the barriers, now called cantori, through which the atoms can diffuse. The diffusion rates of classical and quantum particles are distinctly different, with quantum diffusion being largely suppressed by the cantori [5–11]. The decohering effects of coupling to the environment bring the behaviour of the quantum ensemble towards the classical limit. The decohering influence of spontaneous emission in the atomic optics realization of the δ-kicked rotor has been observed [12–14], as have the effects of the introduction of noise to this quantum system [14].

2. Our analytical system

The atom interacts with a standing wave of near-resonant light (frequency ω_L) which is temporally modulated with period T. When the detuning $\delta_L = \omega_0 - \omega_L$ (where ω_0 is the resonant frequency of the transition) is sufficiently large compared to the resonant Rabi frequency $\Omega/2$, the amplitudes of the excited states can be adiabatically eliminated because our detunings are large compared to the Rabi frequency [15, 16]. The dynamics are governed by stimulated two-photon scattering between ground states, with momentum changes in units of $2\overline{h}k_L$. Classically, the atom behaves as a dipole in a conservative, one-dimensional potential. The Hamiltonian in this limit is given by

$$\mathcal{H} = \frac{p_x^2}{2M} - \frac{\overline{h}\Omega_{\text{eff}}}{8}\cos 2k_L x \sum_{n=-\infty}^{\infty} f\left(\frac{t}{T} - n\right) \qquad (1)$$

where $f(t/T)$ specifies the temporal shape of the 'kicks', (with $0 \leqslant f(t/T) \leqslant 1$), k_L is the laser wavenumber, and Ω_{eff} is the effective Rabi frequency. For a two-level atom, $\Omega_{\text{eff}} = \Omega^2/\delta_L$ but for our system we instead have $\Omega_{\text{eff}} = \Omega^2(s_{45}/\delta_{45} + s_{44}/\delta_{44} + s_{43}/\delta_{43})$, where the terms in brackets take into account the different dipole transitions between the relevant hyperfine levels in caesium ($F = 4 \rightarrow F' = 5, 4, 3$). Because of the three-dimensional symmetry of the MOT, we have assumed equal populations of the Zeeman sub-levels, yielding numerical values for the s_{4j} of $s_{45} = \frac{11}{27}$, $s_{44} = \frac{7}{36}$, and $s_{43} = \frac{7}{108}$; δ_{4j} are the corresponding detunings. If in the extreme case atoms piled up in the $m = \pm 4$ states, the potential would only increase by 16%. Note that the different magnetic sub-levels will experience different AC Stark shifts. For the smallest detuning used in this work this results in a 5% spread in the coupling strength.

We can write the Hamiltonian in dimensionless form as

$$H = \frac{\rho^2}{2} - k\cos\phi \sum_{n=-\infty}^{\infty} f(\tau - n) \qquad (2)$$

where $k = \overline{h}\Omega_{\text{eff}}k_L^2T^2/2M$ is a measure of the perturbation of the system called the kick strength, $\tau = t/T$, $\phi = 2k_Lx$, $\rho = (2k_LT/M)p_x$, and $H = (4k_L^2T^2/M)\mathcal{H}$. If we consider the dynamics of the laser beam on a single half wavelength, the Hamiltonian is that of a driven rotor, with dimensionless parameters $I = 1$ and $\omega_0^2 = k$, where ω_0 is the small amplitude oscillation frequency of the rotor. In the quantized model, ϕ and ρ are conjugate variables with a commutation relation $[\rho, \phi] = -\mathrm{i}\bar{k}$, where $\bar{k} = 4\overline{h}k_L^2T/M$ is our scaled Planck's constant.

Experimentally, we use a double pulse kick (see figure 1). For this $f(\tau)$ the Hamiltonian can alternatively be written as

$$H = \frac{\rho^2}{2} - k\sum_{m=-\infty}^{\infty} a_m\cos(\phi - 2\pi m\tau) \qquad (3)$$

where $a_m = \frac{1}{10}\,\mathrm{sinc}\,\frac{m\pi}{20}\cos\frac{m\pi}{10}$. (With the sinc function defined as $\mathrm{sinc}(x) = \sin(x)/x$.) The rotor is driven by traveling cosine waves, the speed of the mth cosine wave corresponding to a dimensionless momentum of $\rho = 2\pi m$. There will be a primary resonance in the phase space wherever the speed of rotation of the rotor matches the speed of a cosine wave [4]. In the reference frame in which the cosine wave is at rest, the rotor will be trapped in a pendulum potential. This causes a change in the topology of the classical phase space at $\rho = \rho_m$, for $a_m \neq 0$. For m such that $a_m = 0$ there is a missing primary resonance. The widths of the primary resonance zones are given by $\delta\rho_m = 4\sqrt{a_mk}$. The Chirikov condition for overlap is that the spacing between the resonances be equal to the sum of the half-widths or $|\rho_m - \rho_n| = 2\sqrt{a_mk} + 2\sqrt{a_nk}$. Overlap of adjacent resonances is the mechanism for the destruction of KAM tori [4]. We expect tori in the vicinity of missing resonances to survive higher kick strengths than all others. A more sophisticated analysis must take into account the appearance of secondary resonances arising from interactions between the primary resonances.

3. Experimental set-up

Our experimental set-up is very similar to that used in the experiments of Ammann *et al* [12, 13] and Moore *et al* [17]. Approximately 10^5 caesium atoms are trapped and laser cooled in a standard MOT powered by two diode lasers operating in the infrared (852 nm). The initial trapped cloud has a FWHM of 200 ± 20 μm and a temperature of 10–15 μK. The temperature tends to be stable within an experimental run, and the slight day-to-day temperature variations do not affect our results as they correspond respectively to 99.9%

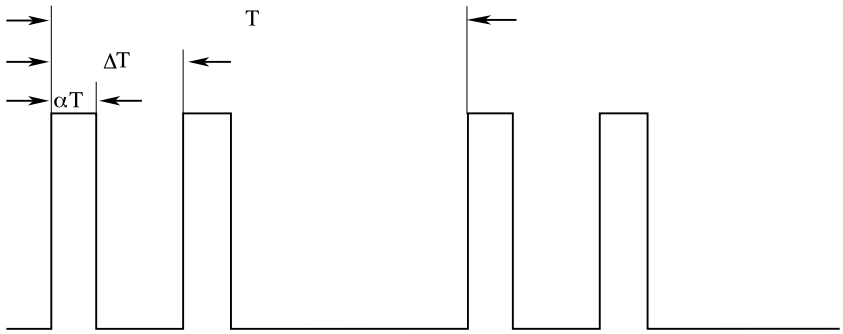

Figure 1. Double pulse showing definitions of α and Δ.

and 99.5% of atoms initially within the phase space bounded by the cantori we are studying. The periodically modulated potential (described in section 2) is provided by a third diode laser. The beam from this laser passes through an 80 MHz acousto-optic modulator (AOM) and a single-mode optical fibre which spatially filters the light and delivers it to the trap. The beam is then collimated and retroreflected from a mirror on the opposite side of the trap to form a standing wave potential across the atomic cloud. The calculated beam waist at the cloud is 800 ± 30 μm. This potential is temporally modulated via the RF supply to the AOM. Our calculated Rabi frequency at the centre of the trap, for maximum optical power is $\Omega/2\pi = 310$ MHz. A reasonably narrow distribution in the kicking strength k is produced by the finite widths of the cloud and the beam waist of the kicking potential (RMS spread of 6% and $k_{\mathrm{mean}} \approx 0.94 k_{\mathrm{max}}$). In the remainder of this paper, k always refers to k_{mean}.

In the system Hamiltonian, the pulse train is described by $f(\tau)$. Any pulse of finite length will create KAM tori in the phase space of the system. They were observed in recent quasi δ-kicked rotor experiments [12, 13, 17] and were discussed in a recent paper by Klappauf *et al* [18]. In these studies, the effects of the KAM tori were avoided by tailoring the pulse length to push them into regions of phase space beyond the localization length of dynamical localization. A pulse train consisting of single pulses is not however the best system for studying the properties of KAM tori and cantori because the only energetic chaotic sea lies between the surviving tori of lowest momentum. Energetic chaotic seas aid the diffusion of particles away from the partially permeable barrier and are important experimentally in isolating the effect of the boundary in phase space. We use a double pulse per kicking cycle where the pulse period is $T = 25$ μs with dimensionless pulse width $\alpha = \frac{1}{20}$ and dimensionless pulse spacing $\Delta = \frac{1}{10}$ (see figure 1). This pulse shape gives energetic chaotic seas on both sides of the long-lived KAM tori with the smallest absolute momentum (see figure 2). To achieve varying levels of spontaneous emission, we varied $\delta_L = \omega_0 - \omega_L$, the detuning of the kicking potential from resonance, while simultaneously altering the beam intensity to maintain a constant kicking strength.

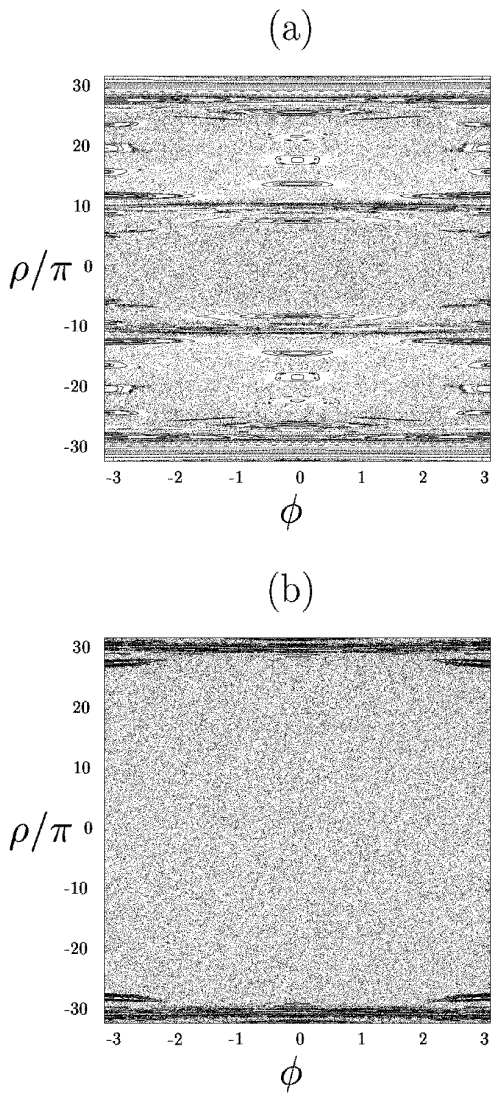

Figure 2. (*a*) The Poincaré section of the system for a very low kick strength. The unbroken KAM tori are clearly visible at $\rho = \pm 10\pi$ and $\pm 30\pi$. (*b*) The same Poincaré section for $k \sim 300$ where the cantori at $\rho = \pm 10\pi$ are no longer visible in the phase space at the resolution of the section.

4. Transport through cantori

Classical particles which are no longer confined to their own tori can diffuse rapidly even through a recently broken cantorus. The cantorus no longer forms an impenetrable barrier in the classical phase space and trajectories from both sides of the original boundary can eventually fill the

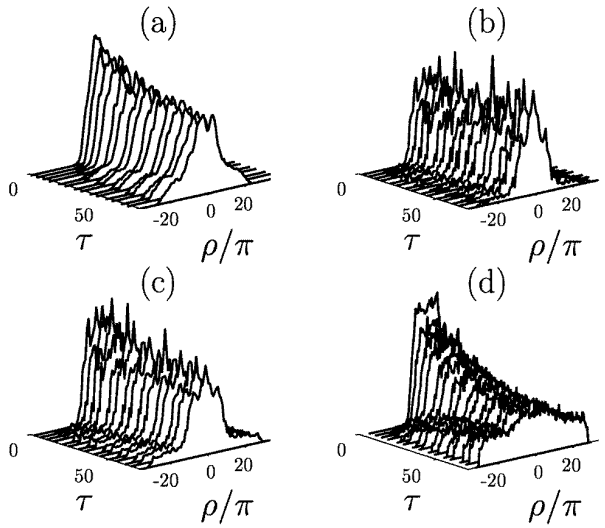

Figure 3. Momentum distributions for a kick strength $k = 280$ as a function of the number of kicking cycles τ. The experimental data (*a*) with its probability of spontaneous emission per cycle $\eta = 0.019$, shows its distinctive shoulders at $\rho = \pm 10\pi$. (*b*) A quantum simulation for the experimental parameters with no spontaneous emission, (*c*) a quantum simulation including spontaneous emission $\eta = 0.019$ and (*d*) the corresponding classical simulation.

entire region between two adjacent, unbroken tori. Quantum particles however behave very differently. Various numerical studies of particle transport through cantori [5–9] have shown that, until the phase space area escaping through the cantori per kick cycle was $\sim\overline{h}$, the diffusion of quantum particles is restricted to a quantum tunnelling-like behaviour i.e. there will be a distinct difference between the diffusion rates of classical and quantum particles. This has recently been confirmed experimentally [10, 11]. Figure 2(*a*) shows a Poincaré section of our system for a very low kicking strength. The KAM tori at $\rho = \pm 10\pi$ and $\pm 30\pi$ are clearly visible as regions of stability between large chaotic seas. Figure 2(*b*) shows the Poincaré section for $k \sim 300$, which is comparable with the kicking strengths used in our experimental work. The tori at $\rho = \pm 10\pi$ are no longer visible in the phase space at this resolution; however they have been shown to still have a significant effect on the dynamics of both the quantum [10, 11] and classical systems.

We prepare our atoms so that they initially lie within the $\rho = \pm 10\pi$ cantori and monitor their subsequent evolution through the boundaries. The final momentum distributions of the atomic cloud display distinctive 'shoulders' at $\rho = \pm 10\pi$ (as shown in figure 3) due to the inhibition of diffusion introduced by the cantori. The quantum simulations show complex structure as a particular initial state was used in the calculation, whereas the experimental distributions are smoother due to unavoidable (albeit small) variations in experimental parameters. The double-peaked structure and the slight asymmetry in the measured line shape are due to interference fringes in the optical molasses. This KAM localization is distinct from the more widely studied 'dynamical localization' (for a discussion see [11]). The signature of dynamical localization is an exponential lineshape in momentum space which is markedly different from the box-like distributions and characteristic shoulders observed with KAM boundaries. Also, for this experiment, the localization length of the system, $l_\rho \sim 170$ is considerably longer than the momentum width of the KAM boundaries at $\rho = \pm 10\pi$ and $\pm 30\pi$ and hence KAM localization occurs before dynamical localization can have an effect.

5. Decoherence

The theory of decoherence provides the most recent and so far perhaps the most satisfying of a series of attempts to explain the disparities between the predictions of quantum mechanics and the everyday experiences of the world we inhabit (see section 1). The field of quantum chaos provides an ideal backdrop for a study of the predicted effects of decoherence. It is now widely accepted that sensitive dependence on initial conditions—the hallmark of classical chaos—does not occur in closed quantum systems. This raises problems for the quantum–classical correspondence (QCC) principle. Quantum mechanics must be able to describe the classical limit of chaotic behaviour. In this case, employing the limit as $\overline{h} \rightarrow 0$ is not entirely satisfactory. Chaotic systems can develop highly complex phase space structures in logarithmically short times and hence the small but non-zero value of $\overline{h}$ is an important factor.

According to the work of Zurek *et al* [2, 3], these difficulties in restoring the classical behaviour can be eliminated by realizing that it is not possible to isolate macroscopic quantum systems from their environment. The coupling of the extraneous degrees of freedom of a system to the environment destroys the quantum coherences on a timescale inversely proportional to the degree of coupling. In our experiments and simulations, we introduce coupling via spontaneous emission induced by the kicking potential. As the level of spontaneous emission increases, so does the coupling of the system to the vacuum fluctuations which constitute the environment. The predicted effect of this increased coupling is an increase in the transport of quantum particles across the cantori as the quantum diffusion rate tends to its classical limit. For the purposes of simulation we note that $H = \rho^2/2 - k\cos\phi = H_{\text{light}}$ while the driving potential is 'switched on', and $H = \rho^2/2 = H_{\text{dark}}$ otherwise. Classical trajectories involve periods of pendulum motion described by Jacobi elliptic functions, alternating with periods of free evolution. Usually 10^4 trajectories are followed during each run. For each pulse, the amplitude and phase of the elliptic function is matched to the position and motion of each trajectory by inverting the elliptic function numerically. To simulate our experiments, we choose our initial conditions randomly from a thermal distribution. To produce Poincaré sections, more uniform conditions are chosen, and optimized to reveal the phase space structure.

The quantum system is represented by a basis of $N = 128$ momentum eigenstates $|n\rangle$, where $\rho|n\rangle = n\hbar|n\rangle$ and $n = -64, \ldots, 63$. For our parameter values, the duration of each laser pulse is $\frac{1}{20}$ of the total cycle period (see figure 1).

The evolution operator for a double kick cycle is

$$U = \exp\left(-\mathrm{i}\frac{17H_{\mathrm{dark}}}{40\bar{k}}\right)\exp\left(-\mathrm{i}\frac{H_{\mathrm{light}}}{20\bar{k}}\right)\exp\left(-\mathrm{i}\frac{H_{\mathrm{dark}}}{20\bar{k}}\right) \times \exp\left(-\mathrm{i}\frac{H_{\mathrm{light}}}{20\bar{k}}\right)\exp\left(-\mathrm{i}\frac{17H_{\mathrm{dark}}}{40\bar{k}}\right) \quad (4)$$

where $\langle m|H_{\mathrm{dark}}|n\rangle = \frac{1}{2}n^2\bar{k}^2\delta_{m,n}$, $\langle m|H_{\mathrm{light}}|n\rangle = \frac{1}{2}n^2\bar{k}^2\delta_{m,n} - \frac{1}{2}k(\delta_{m,n+1} + \delta_{m,n-1})$ and we treat n as periodic. The $N \times N$ matrices are exponentiated numerically. In the case of evolution without spontaneous emission, the evolution is entirely coherent, and is solved by finding the eigenvectors of the evolution operator (Floquet method). For incoherent evolution, the effects of spontaneous emission are simulated by adding the density matrix to two shifted versions of itself, once per kick:

$$\langle m|\hat{\mathcal{P}}|n\rangle = \tfrac{1}{2}\eta(\langle m+1|\hat{\mathcal{P}}|n+1\rangle + \langle m-1|\hat{\mathcal{P}}|n-1\rangle) + (1-\eta)\langle m|\hat{\mathcal{P}}|n\rangle \quad (5)$$

where $\hat{\mathcal{P}}$ is the density operator and η is the probability for a particular atom to spontaneously emit during one kick cycle. In a previous study by our group, we calculated the effect of spontaneous emission in the δ-kicked rotor through a Monte Carlo wavefunction calculation [12]. The approximate way in which we account for spontaneous emission in this paper produces results which are negligibly different from the Monte Carlo wavefunction calculation, but are significantly more computationally efficient.

A convenient way to visualize the information represented by the density matrix is in the form of a Wigner function. For a discrete, truncated basis we use the toroidal Wigner function as defined in [19],

$$w(X_k, P_l, t) = \sum_{j=0}^{2N-1}\exp\left(\mathrm{i}\frac{\pi jk}{N}\right)\frac{1+(-1)^{l+j}}{2} \times \left\langle\frac{l+j}{2}\right|\hat{\mathcal{P}}\left|\frac{l-j}{2}\right\rangle \quad (6)$$

where $P_l = (\bar{k}/2)l$ and $X_k = \pi k/N$. This gives a Wigner function defined on a $2N \times 2N$ grid. Averaging over cells of four adjacent points we reduce the grid to $N \times N$. This was implemented in `Matlab` using a fast Fourier transform algorithm. Examples of results obtained are shown in figure 4. We see that decoherence smoothes the Wigner function, removing the rapid oscillations and negative regions which are characteristic of quantum interference phenomena.

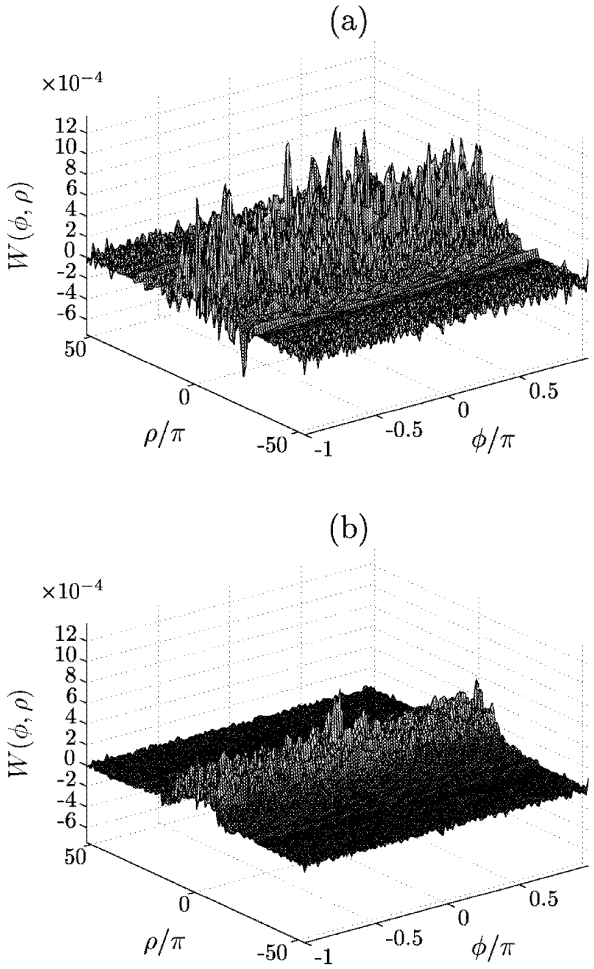

Figure 4. Wigner functions for the system after 70 kicks, with $k = 280$. (*a*) Corresponds to a probability of spontaneous emission per kick cycle $\eta = 0$, giving pure quantum evolution. We see rapid fluctuations and negative regions, indicating quantum interference effects. (*b*) Results for $\eta = 0.02$, comparable with experimental value. Quantum effects are reduced leading to a more classical distribution.

6. Experimental results

In the absence of decoherence, the caesium atoms behave as quantum particles. Thus even for cantori where significant diffusion of classical particles can occur, our quantum particles should still be strongly contained as can be seen from our classical and quantum simulations in figure 5 where we calculate the percentage of atoms that cross the $\rho = \pm 10\pi$ cantori as a function of the number of kick cycles. Not until the phase space escaping through the cantorus per cycle is $\sim\bar{h}$, or in our scaled units $\sim\bar{k}$, do the quantum particles move to any great extent across the boundary. For our experimental parameters, the phase space flux through the $\rho = \pm 10\pi$ cantori per kicking cycle is $\sim 4.6\bar{k}$ so the quantum diffusion will be inhibited. The predicted effect of increasing the coupling to the environment then is to increase the transfer of atoms across the cantorus. As the quantum system becomes more and more strongly coupled to its environment, the behaviour of the atoms is expected to approach the classical limit of rapid diffusion.

Our experimental results support this prediction (see figure 6). For a given kick strength, we compare the system for $\delta = 2.8$ GHz and $\delta = 1.0$ GHz. The lower limit on the detuning is imposed by the approximation made in our numerical calculations that the excited state of the atoms can be adiabatically eliminated (see section 2). The upper limit (2.8 GHz) is mainly due to optical power restrictions from our diode laser—as the detuning increases, the intensity must also increase to maintain a constant kicking strength.

As the detuning decreased, the percentage of particles outside the $\rho = \pm 10\pi$ cantori increased and the experimental curve rose towards the classical prediction. Our results also show reasonable agreement with our quantum mechanical simulations which included the effects of spontaneous

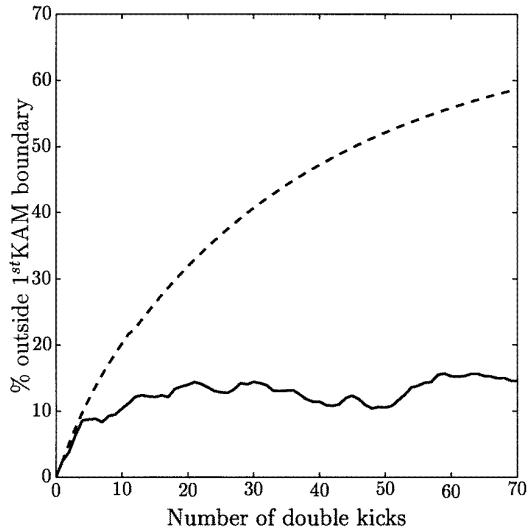

Figure 5. Quantum (solid) and classical (dashed) simulations for a kicking strength of $k = 270$ showing the percentage of atoms to cross the $\rho = \pm 10\pi$ cantori. This graph clearly shows the inhibition to quantum diffusion presented by the cantorus.

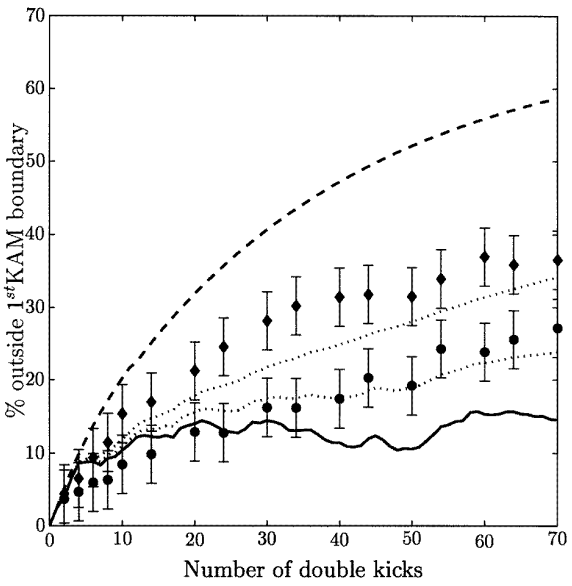

Figure 6. Percentage of particles to cross the $\rho = \pm 10\pi$ cantori. Experimental results for $\eta = 0.02$ (●) and $\eta = 0.05$ (♦) all at a kicking strength of $k = 270$. Quantum simulations for the experimental parameters are shown as dotted lines. The classical simulation (dashed) and quantum simulation with zero spontaneous emission (solid) are shown for comparison. The error bars represent our ±4% measurement uncertainty.

emission. The main sources of error are the measurement of optical beam power and the finite resolution of the CCD camera. The resolution of our CCD (19 pixels mm^{-1}), coupled with our 12 ms expansion time, allowed us to determine the position of the momentum line to an accuracy of $\Delta\rho = \pm 0.8$. At our kick strength of $k = 270$, this results in an uncertainty in our measured probability of ±4%. The 6% variation in the kicking strength k is sufficiently small so as not to contribute an appreciable variation in the lineshapes. We repeated our experiment a number of times during each experimental session, and the resulting spread in our measured values of ±4% is reflected in the error bars in figure 6. In this figure, we see good agreement between experiment and theory for the 2.8 GHz detuning, while for 1.0 GHz there is only reasonable agreement which is probably due to absolute uncertainty in the light power level and detuning values.

As one can see from figure 6, the increase in the spontaneous emission rate causes the behaviour of this ensemble of quantum particles to approach the behaviour of a classical ensemble. Our experimental set-up does not permit us to force our atoms to this limit, as we are limited by laser power and the adiabatic elimination approximation. However, our quantum simulations reveal that further increases in the spontaneous emission rate allow the quantum ensemble to mimic the classical. All our measurements were at a fixed 'Planck's constant' of $\bar{k} = 2.6$; the consequences of a variation of $\bar{k}$ in this double pulse system will be the subject of future work. Suffice it to say that decreasing $\bar{k}$ brings the ensemble closer to the fully classical representation.

7. Conclusion

Using laser-cooled caesium atoms, we have observed the controlled decoherence of a real quantum system via coupling to the environment. This adds to the previous work on decoherence through the atom optics realization of the δ-kicked rotor and also the experiments of Haroche *et al* [20] and Wineland *et al* [21]. We have demonstrated that the quantum diffusion rate tends towards the classical rate with an increasing degree of decoherence. The introduction of decoherence via spontaneous emission increases the rate of transport of atoms across the cantori and alters the characteristic shape of the KAM localized distribution such that it tends towards the classical (uniform) distribution.

The link between the quantum domain and the familiar classical world remains a hotly debated topic. The quantum–classical correspondence principle requires that quantum mechanics contains the classical macroscopic limit. It appears that environment induced decoherence can help in the understanding of QCC. This interpretation is authenticated via the results presented in this paper, as well as previous studies of decoherence in the atomic optics manifestation of the δ-kicked rotor [12–14]. We note that while we can make our ensemble of caesium atoms behave like an ensemble of classical particles, we do not infer that there is any degree of chaos in the presented quantum system.

We have experimentally confirmed that a cantori can inhibit the motion of a quantum particle [10,11]. In this paper we observe that decoherence introduced via spontaneous emission markedly changes the diffusive behaviour of the caesium atoms that we subject to our tailored kick series. An increase in the spontaneous emission rate diminishes the effect of cantori localization in the quantum system, and diffusion similar to that predicted classically is observed.

Acknowledgments

This work was supported by the Royal Society of New Zealand Marsden Fund and the University of Auckland

Research Committee. The authors would like to thank Dan Walls and other members of the University of Auckland Quantum Optics group for useful discussions, guidance and encouragement throughout the course of this research.

References

[1] Zurek W H 1998 *Preprint* quant-ph/9802054
[2] Zurek W H and Paz J P 1994 *Phys. Rev. Lett.* **72** 2508
[3] Zurek W H 1991 *Phys. Today* **44** 36
[4] Reichl L E 1992 *The Transition to Chaos In Conservative Classical Systems: Quantum Manifestations (Institute for Nonlinear Science)* (New York: Springer)
[5] Geisel T, Radons G and Rubner J 1986 *Phys. Rev. Lett.* **57** 2883
[6] Geisel T and Radons G 1989 *Phys. Scr.* **40** 340
[7] Brown R C and Wyatt R E 1986 *Phys. Rev. Lett.* **57** 1
[8] MacKay R S and Meiss J D 1988 *Phys. Rev.* A **37** 4702
[9] MacKay R S, Meiss J D and Percival I C 1984 *Physica* D **13** 55
[10] Christensen N, Ammann H, Ball G and Vant K 1999 *Laser Phys.* **9** 281
[11] Vant K, Ball G, Ammann H and Christensen N 1999 *Phys. Rev.* E **59** 2846
[12] Ammann H, Gray R, Shvarchuck I and Christensen N 1998 *Phys. Rev. Lett.* **80** 4111
[13] Ammann H, Gray R, Christensen N and Shvarchuck I 1998 *J. Phys. B: At. Mol. Opt. Phys.* **31** 2449
[14] Klappauf B G, Oskay W H, Steak D A and Raizen M G 1998 *Phys. Rev. Lett.* **81** 1203
[15] Dalibard J and Cohen-Tannoudji C 1985 *J. Opt. Soc. Am.* B **2** 1707
[16] Graham R, Schlautmann M and Zoller P 1992 *Phys. Rev.* A **45** R19
[17] Moore F L, Robinson J C, Bharucha C F, Sundaram B and Raizen M G 1995 *Phys. Rev. Lett.* **75** 4598
[18] Klappauf B G, Oskay W H, Steck D A and Raizen M G 1999 *Physica* D at press
[19] Kolovsky A R 1996 *Chaos* **6** 534
[20] Brune M, Hagley E, Dreyer J, Maître X, Maali A, Wunderlich C, Raimond J M and Haroche S 1996 *Phys. Rev. Lett.* **77** 4887
[21] Monroe C, Meekhof D M, King B E and Wineland D J 1996 *Science* **272** 1131